Jinnouchi *et al.*
Journal of Analytical Science and Technology (2024) 15:12
https://doi.org/10.1186/s40543-024-00423-7

Journal of Analytical Science and Technology

RESEARCH ARTICLE

Open Access

New development of compact magnetic separator for on-site material screening in various geological survey

So Jinnouchi[1*], Chiaki Uyeda[1], Keiji Hisayoshi[1], Gen Takayama[2] and Kentaro Terada[1]

Abstract

Magnetic separation has been recognized as a valuable technique for extracting or separating target materials from mixed heterogeneous particles. In conventional geological research, it has been used to separate ferro- and ferrimagnetic minerals such as Fe–Ni metal, magnetite and ilmenite. Recently, a mixture of diamagnetic and weak paramagnetic particles has been successfully separated into groups of different materials using a compact magnetic circuit; however, the resolution was not sufficiently high to analyze various heterogeneous particles studied in geological research. Here, we show that the resolution has remarkably improved by developing new magnetic separator. Accordingly, the separation efficiency of particles due to magnetic translation increased by a factor of ~ 2.5, and two different materials were definitely resolved when their variance of the magnetic susceptibility exceeded ~ 2×10^{-7} emu/g; previously, limit of the resolution was above 7×10^{-7} emu/g. We also established the orbit simulation program in magnetic and gravitational field, which accurately predicted the actual trajectory due to magnetic translation. The improved separation resolution of the new separator has significantly increased the range of solid materials that can be magnetically separated, and the range of applications has been considerably expanded to include the matrix of primitive meteorites, surface soils of solid planets and satellites, volcanic ash and sedimentary rocks. The newly developed device is compact and requires little electric power, allowing on-site material screening in various geological research.

Keywords Magnetic separation, Magnetic circuit, Microplastic

Introduction

The magnetic separation technique for various heterogeneous samples has been primarily used to extract or eliminate ferromagnetic materials and strong paramagnetic materials, whereas it was generally difficult to separate weak magnetic (i.e., diamagnetic and weak paramagnetic) materials by a low field intensity generated by permanent magnets. Therefore, a method has been developed to efficiently extract or eliminate a target material by attaching magnetic beads (or magnetic ions) or magnetic ions to the sample (Uhlen et al. 1989). These conventional techniques of magnetic separations have been performed under normal gravity conditions.

Recent experiments performed in microgravity have shown that geological samples composed of weak magnetic materials, such as ice, oxide minerals, volcanic glasses, fossil pollen, and synthetic resins, translate at practical field intensity below 1 T (Uyeda et al. 2010; Hisayoshi et al. 2016; Hitomi et al. 2020; Yamaguchi et al. 2020). Later, magnetic translation and separation of weak magnetic particles were achieved under normal gravity conditions (Uyeda et al. 2019; Jinnouchi et al. 2022).

*Correspondence:
So Jinnouchi
jinnouchi@ess.sci.osaka-u.ac.jp
[1] The Department of Earth and Space Science, Graduate School of Science, Osaka University, 1-1 Machikaneyama-cho, Toyonaka-Shi, Osaka 560-0043, Japan
[2] Department of Physics, Graduate School of Science, Osaka University, Toyonaka-shi, Osaka 560-0043, Japan

In these experiments, translation was observed using a high-speed camera, and it was confirmed that the particles were translated by a composition of gravity and magnetic force. Here, it is noted that the two forces are both mass-dependent.

These prescient findings provide new insights into earth and planetary science, because the new technique of magnetic translation could be used as a pretreatment technique to comprehensively analyze the materials included in an aggregate of heterogeneous particles; it is noted that most samples studied in geology and space science are heterogeneous particles with different origins (Anders. 1964; Papike et al. 1982; Javaux. 2019). Hence, the new method of magnetic separation might play the role of a "chromatographic technique" specified for solid particles (Uyeda et al. 2019). However, the resolution of magnetic separation was insufficient for practical applications, such as preprocessing of mixtures (e.g., regolith) in earth and planetary science.

In this study, a new magnetic circuit operated under normal gravity was designed and fabricated to improve the resolution of material separation to a practical level. Two attempts were made to improve the performance of the circuit, and the achieved resolution was examined by separating various diamagnetic particles with different χ's, where χ denotes magnetic susceptibility per unit mass. A calculation program was developed to reproduce the trajectory of magnetic translation in the magnetic and gravitational fields for the first time, and the efficiency of a dynamic equation was quantitatively examined.

Experiment

In the present study, the size of the device containing the magnetic circuit was kept below 10 cm in diameter and weighed less than 2 kg, in order to realize a mobile magnetic separator. As shown in Fig. 1, the magnetic field to generate repulsive magnetic force in the diamagnetic particle was mainly generated by a cubic FeNdB block (4.0×4.0×4.0 cm) described on the left side of the figure, and an experiment of magnetic translation was performed inside the gap located in the right side of the FeNdB cube. To increase the magnetic field intensity B and the field gradient (dB/dx) inside the gap, the yoke was doubled, and the width of the magnetic pole was narrowed to 0.8 cm; in the conventional apparatus, the width was as large as 2.0 cm. The yoke consisted of two pairs of soft magnetic iron plates, 10 cm long, 4 cm high, and 1 cm thick. The entire device was covered with

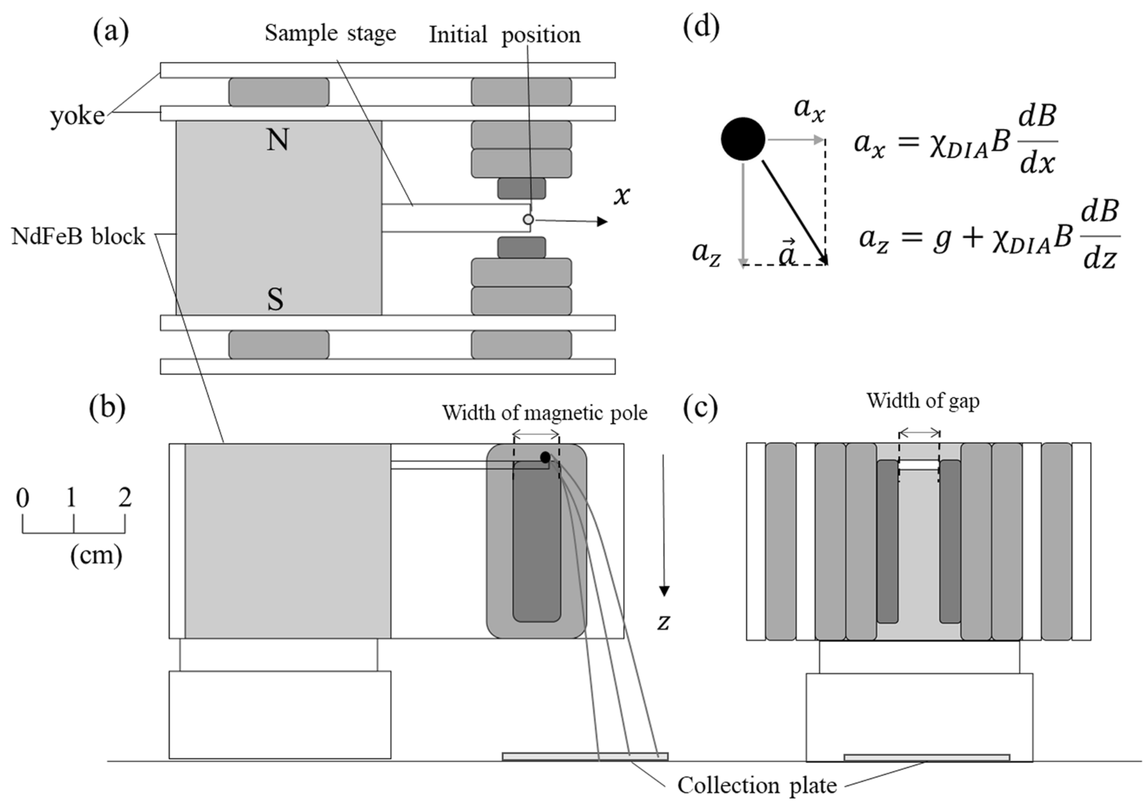

Fig. 1 Schematic view of the setup to magnetically separate heterogeneous diamagnetic minerals, **a**, **b** and **c** in the figure denote top, side and front view, respectively. The geometric relationship of acceleration caused by magnetic force and gravity is shown in **d**

a 0.5 mm thick iron plate to reduce the leakage of magnetic field lines and to confine the magnetic field within the magnetic circuit. The space in the gap area is 0.8 cm wide, 4 cm high, and the gap width is 0.6 cm.

Table 1 Experimental results, relationship between susceptibility and translation distance of present and previous study (Jinnouchi et al. 2022)

Materials	$\chi_{DIA} \times 10^{-7}$ (emu/g)	Distance (mm) (present)	Distance (mm) (previous)
[a] Gold: Au	−1.42	−0.19	–
[d] Silicon Carbide: SiC	−3.19	6.6	–
[c] Alumina: Al2O3	−3.63	11	–
Diamond: C	−5.88	–	3.3
[b] Polypropylene:C3H6	−7.6	15	–
[a] Bismuth: Bi	−13	17	6.4
[a] Graphite: C	−52.0	38	15

[a] Gold, bismuth and graphite were purchased from Nilaco Co (Tokyo, Japan).
[b] Polypropylene was purchased from Polysciences Inc (Warrington, PA, USA).
[c] Synthetic sapphire was purchased from Nakazumi Co (Japan). [d] SiC from Nakarai Tesque Co (Kyoto, Japan)

Six samples were prepared for the experiment; their numerical details are listed in Table 1. Gold, bismuth, graphite, silicon carbide and corundum used in the experiment were synthetic diamagnetic materials. After preparing sub-mm-sized samples, they were dispersed in ethanol and used in an ultrasonic cleaner for approximately 15 min. The sample size was kept between mm and sub-mm because the optimum area for releasing the sample was narrow. Accordingly, the resolution of magnetic separation would be improved by controlling the sample size within a limited range. The initial position of the particles on the sample holder was set at the position where the sample obtained the maximum magnetic force $\left(\frac{m\chi BdB}{dx}\right)$ to attain maximum acceleration. This position was determined from the spatial distribution of $B(x)$ in the experimental area, measured using a Gauss meter (F.W. BELL Co, MODEL 5080).

Before the experiment, the sample, magnetic separation device, and experimental apparatus were neutralized by an ionizer (HOZAN, F-93) for one hour. In a magnetic separation experiment, particles with different magnetic susceptibilities were set on a sample

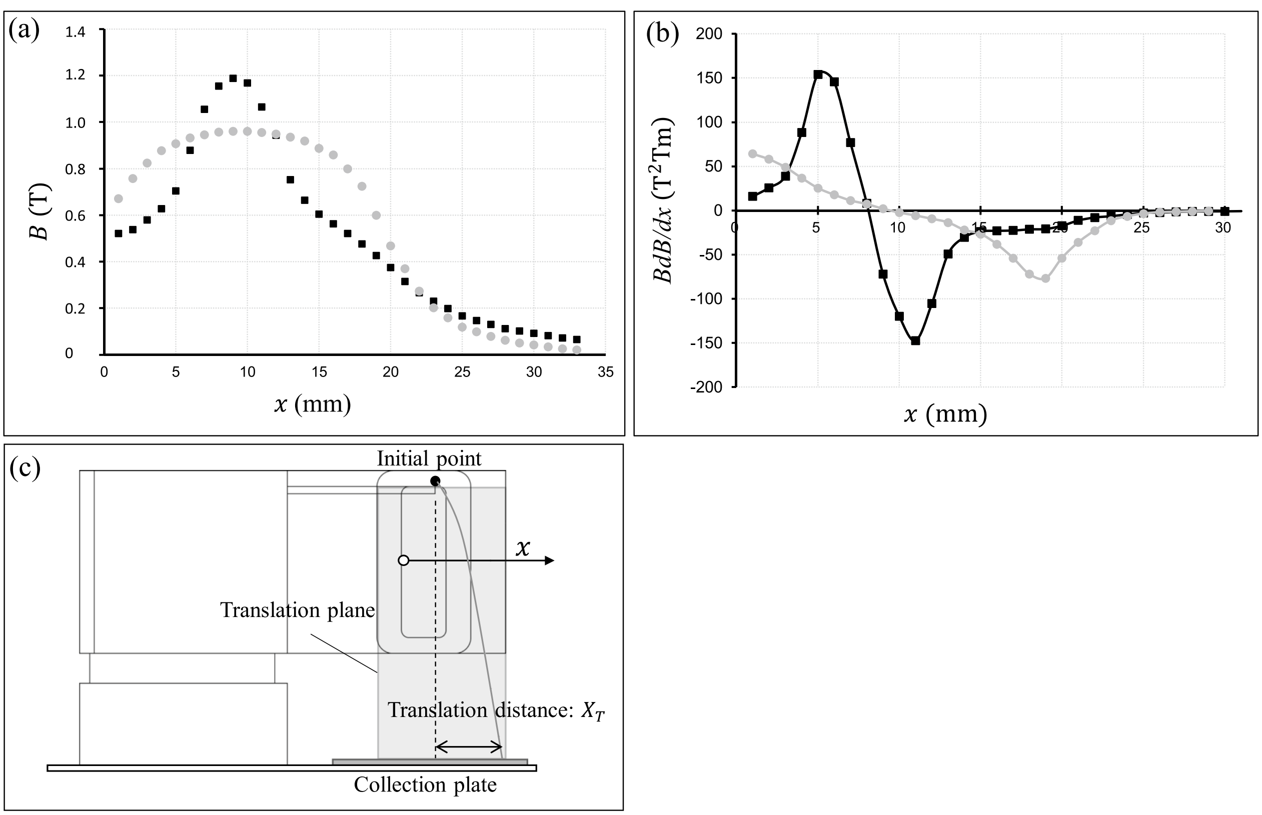

Fig. 2 Magnetic field (**a**) and *BdB/dx* (**b**) distribution generated by the setup described in Fig. 1. Magnetic field measured along a broken line described in **c**. Black squares and gray circles denote present and previous studies, respectively

holder and released with a small initial velocity; the particles proceeded in an area denoted as a "Translation Plane" in Fig. 2c, which is included in the center plane of the gap, parallel to the xz plane. Translated particles reached the collection plate described in Figs. 1b, c and 2c. As shown in Fig. 2c, horizontal separation of a particle due to the magnetic translation was determined by separation of particles observing the collection plate defined as X_T; here, the x-coordinate of the initial sample position was defined as $X_T = 0$.

As mentioned above, in order to improve the resolution of the magnetic separation in the present study, both the magnetic field and the magnetic field gradient were increased compared to the device used in a previous study (Jinnouchi et al. 2022). As a result, the maximum magnetic field of the improved device was increased from 0.9 to 1.2 T, and the product of magnetic field and magnetic field gradient was significantly improved from 72 to 150 T^2/m.

A calculation program was designed and constructed for the purpose of reproducing the trajectory of the aforementioned magnetic translation that proceeded in the translation plane. The program was based on a field distribution produced by the magnetic circuit developed in the previous study. The experimental X_Ts obtained in the aforementioned manner for individual particles were compared with the results of the calculations.

In the program, gravitational acceleration was applied in the $+z$ direction (see Fig. 2c), whereas acceleration caused by magnetic force was applied in the $+x$ direction. The numerical program defines the coordinates of the sample every single microsecond to derive the flight trajectory. The calculation procedure is as follows: (1) The translation plane is divided into 1-mm meshes $[x = x_i, z = x_j]$ in which the particles exhibit quasi-parabolic motion. (2) Constant values of the magnetic field $B = B\ (x_i, z_j)$ are defined inside individual meshes $[x = x_i, z = x_j]$, where $B = \left[B_x(x_i, z_j), B_y(x_i, z_j), B_z(x_i, z_j)\right]$ for each mesh was measured by the aforementioned Gauss meter. From the variances of measured B and field gradient dB/dx between adjacent meshes defined at $[x = x_i, z = z_j]$ and $[x = x_{i+1}, z = z_j]$, acceleration $\boldsymbol{a}$ of a particle that is translating between the two meshes is obtained. A relationship $(a_x, a_z) = (\chi B dB/dx, g + \chi_{DIA} B dB/dz)$ is used in the above calculation; the relationship is deduced in Eqs. (1) and (2). (3) Assuming the initial position of the particle as $r_0 = (x_0, z_0)$ and the initial velocity as zero, we proceeded with a calculation based on a conventional energy conservation described as $1/2\ m[v(x_i)^2 - v(x_{i+1})^2] = 1/2 m\chi[B(x_i)^2 - B(x_{i+1})^2]$ (Hisayoshi et al. 2016; Uyeda et al. 2019).

The deceleration of sample due to the viscous resistance of air is proportional to R^{-2}; R denotes radius of sample. In this current setup, R is 2 orders of magnitude larger (mm size) than in a previous study (Watanabe et al. 2004), and therefore the effect of deceleration caused by the viscous resistance is negligibly small.

Results

When a diamagnetic particle is released in an area where the magnetic field monotonically decreases in one direction, the magnetic repulsive force acting on the particle is proportional to the particle mass m [g] and intrinsic magnetic susceptibility χ_{DIA} [emu/g] of the material. Therefore, in a common area of the magnetic field distribution, that is, the translation plane, as shown in Fig. 2c, the horizontal acceleration of the sample particle in the plane uniquely depends on χ_{DIA}, whereas the vertical acceleration a_z is due to terrestrial gravity and field gradient $a_z = g + \chi_{DIA} B dB/dz$. Therefore, the translation of a diamagnetic particle is determined by two equations of motion which are assumed in the horizontal and vertical direction:

$$[\text{horizontal}] : F_x = ma_x = m\chi_{DIA} B \frac{dB}{dx} \quad (1)$$

$$[\text{vertical}] : F_z = ma_z = mg + m\chi_{DIA} B \frac{dB}{dz} \quad (2)$$

Acceleration vector $\boldsymbol{a}$ of the translating particle is described as

$$\boldsymbol{a} = (a_x, a_z) = \left(\chi_{DIA} B \frac{dB}{dx},\ g + \chi_{DIA} B \frac{dB}{dz}\right) \quad (3)$$

It is noted that $\boldsymbol{a}$ is independent of the mass of the particle because m is canceled out on both sides of Eqs. (1) and (2), and solid particles composed of the same material translate along a common quasi-parabolic trajectory when released at a common initial point in the translation plane. This is because the variance of F_x uniquely occurs by that of χ_{DIA}, and an intrinsic χ_{DIA} is assigned to individual solid material, as listed in Table 2. This means that an ensemble of heterogeneous particles is separated into different groups of materials when they are released at the abovementioned identical position. The experiment of magnetic translation was performed for the five samples listed in Table 1, and the X_T values are determined from the photograph shown in Fig. 3b. As described in Fig. 4, the sequences of magnitudes of X_T's observed in the five samples are consistent with those of published χ_{DIA}'s of the five samples.

Table 2 Magnetic susceptibility of major organic and inorganic materials

Materials	$\chi_{DIA} \times 10^{-7}$ (emu/g)
(Organic materials)	
Alanine: C3H7NO	−5.6
Anthracene: C14H10	−7.2
Cellulose: (C6H10O5)n	−5.7
Methane: CH4	−8.00
Naphthalene: C10H8	−7.08
Polypropylene: C3H6	−7.6
Polystyrene: (C8H8)n	−6.9
Proline: C5H9NO2	−6.0
Urea: CH4N2O	−5.6
(Inorganic materials)	
Alumina: Al2O3	−3.63
Bismuth: Bi	−13
Calcite: CaCO3	−3.55
Carbon dioxide: CO2	−4.77
Diamond: C	−5.88
Enstatite: MgSiO3	−4
Forsterite: Mg2SiO4	−3.3
Graphite: C	−52.0
Ice Ih: H2O	−6.8
Magnesia: MgO	−2.6
Quartz: SiO2	−3.7 to −4.7
Silicon Carbide: SiC	−3.19
Silver: Ag	−1.9
Water: H2O	−7.02

Gupta (1983), Hisayoshi et al. (2016)

From "Magnetic separation of general solid particles realized by a permanent magnet" https://www.nature.com/articles/srep38431

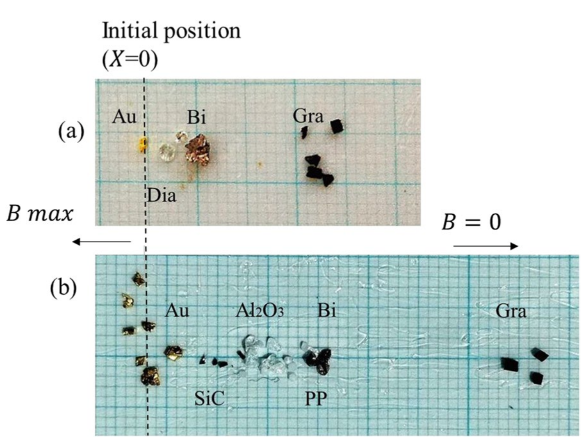

Fig. 3 Images of the collecting plate of the previous study (Jinnouchi et al. 2022) (**a**) and this study (**b**) after the separating heterogeneous diamagnetic particles. Gra, Dia and PP denote graphite, diamond and polypropylene, respectively

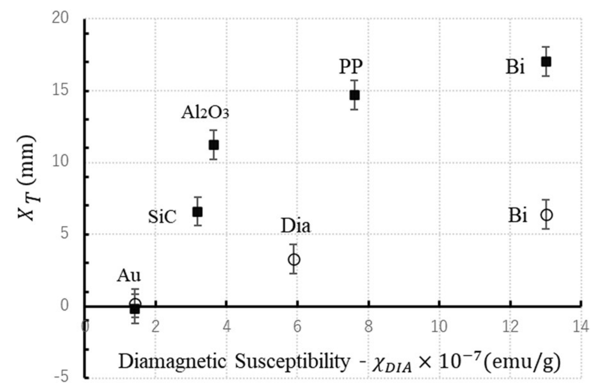

Fig. 4 Compared relationship between χ_{DIA} and X_T obtained from the collecting plate in shown experiment. Black squares and gray circles denote present and the previous studies (Jinnouchi et al. 2022), respectively

Discussion

In order to quantitatively describe the resolution of material separation achieved by the present device, we define a variance of published χ_{DIA}'s between two materials as $\delta\chi$. According to Fig. 3a, the positions of Au and SiC particles on the collection plate are completely separated, and $\delta\chi$ between Au and SiC is $\delta\chi_{A-S} = 1.77 \times 10^{-7}$ emu/g (see Table 2). In comparison, the positions of SiC and Al_2O_3 on the plate partially overlap, and $\delta\chi$ between the two materials is 0.44×10^{-7} emu/g, which is below $\delta\chi_{A-S}$. Hence, the observed result of the collection plate indicates that two materials are completely separated if $\delta\chi$ is above $\delta\chi_{\mathrm{Th}} \sim 2 \times 10^{-7}$ emu/g. (This estimation is effective in the range of $\chi = 0$ to -7.0×10^{-7} emu/g.) It is noted that using the device developed in a previous study (Jinnouchi et al 2022), the lower limit of $\delta\chi$ to achieve complete material separation was as large as ~ 7×10^{-7} emu/g (see Fig. 3a). Thus, the present resolution to separate two different materials has improved by more than a factor of 3 in $\delta\chi$ values, as compared to the previous study.

As described in Fig. 5, the trajectories of particles in the translation plane for gold, diamond, bismuth, and graphite, which were measured in the previous study (Jinnouchi et al. 2022), were reproduced by the calculation program described in "Experiment" section. The predicted X_T were consistent with the observed results for the four samples within the range of experimental errors. This consistency shows that the translation of the particles is almost driven by the magnetic force described in Eqs. (1) and (2), whereas the contributions of other external forces are small.

The calculated trajectories of the particles will also be effective in improving the resolution of the separation in future studies. Specifically, the trajectory of particles in the "Translation Plane" can be numerically predicted

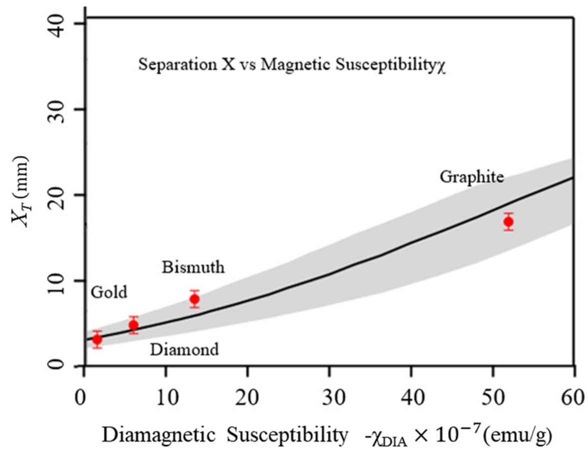

Fig. 5 Relation between magnetic susceptibility χ_{DIA} and magnetic translation distance X_T for diamagnetic particles. Red circles represent the previous experimental results and solid lines represent numerically calculated flying distances. The gray hatch represents the numerically calculated flying distance for an initial position of ± 1 mm

prior to the experiment. The calculation is also effective in optimizing the magnetic circuit for the practical operation of material separation.

It should be emphasized that the improvements of the magnetic circuit in this study have drastically improved the ability to sort particles in the magnetic susceptibility range of ~ $(-1$ to $-10) \times 10^{-7}$ emu/g as shown in Fig. 4. This improvement could potentially expand its application to geochemical exploration. The new separator is usable in obtaining a histogram of materials included in an ensemble of heterogeneous geological samples. It can be used in performing a "hypothesis-free analysis" on the regolith samples returned from the surface of various solid bodies in the solar system, including the asteroids and comets. For example, it is known that lunar regolith which mainly consists of diamagnetic materials such as plagioclase, pyroxene, olivine, silica (Papike et al. 1982), of which χ emu/g are $(-2.2$ to $-4.1) \times 10^{-7}, -4$ $(-4.0$ to $-4.2) \times 10^{-7}, -3.3$ $(-3.7) \times 10^{-7}$ and -3.7 to -4.7×10^{-7} emu/g, respectively; it is noted that susceptibilities in Table 3 and brackets were calculated based on Pascal's additive law (Pople 1962; Bain and Berry 2008), which may differ from actual measured values due to crystal structure and/or trace element concentrations. Hence, our innovative methods have the potential to efficiently enrich quartz and/or ilmenite without the need for electrical power or chemical treatment on the Moon. Consequently, the groundbreaking separation method that we propose have the potential to introduce a new paradigm in on-site lunar resource science.

The proposed separation method using a low-cost permanent magnet can also be applied to the

Table 3 Calculated magnetic susceptibility of major minerals of plagioclase, pyroxene and olivine

Materials	$\chi_{DIA} \times 10^{-5}$ (emu/mol)	$\chi_{DIA} \times 10^{-7}$ (emu/g)
(Plagioclase)		
Anorthite (CaAl2SiO8)	−11	−2.2
Albite (NaAlSi3O8)	−11	−4.0
Orthoclase (KAlSi2O8)	−11	−4.1
(Pyroxene)		
Enstatite (Mg2Si2O6)	−8.0	−4.0
Wollastonite (Ca2Si2O6)	−9.0	−4.2
(Olivine)		
Forsterite (Mg2SiO4)	−5.2	−3.7

Susceptibility of Table 3 was calculated based on Pascal's additive law and may differ from actual measured values

extraction of precious materials as well as the removal of pollutants which are vital industrial and environmental problems. It was suggested that FeNdB magnetic separation offers a promising approach for resource exploration of rare metallic materials such as gold, indium $\left(\chi = -1.1 \times 10^{-7} \text{emu/g}\right)$, platinum $(\chi = +9.8 \times 10^{-7} \text{emu/g})$ or niobium bearing particles in a hazardless manner (Uyeda et al 2019). In addition, it can also be applied to the removal of microplastics in soil, as the minerals that compose soil and sea sand are mostly paramagnetic and subject to magnetic attraction, whereas synthetic plastics are completely diamagnetic and subject to magnetic repulsion (Table 2). Therefore, microplastics included in the soil can be easily removed by utilizing the large variance in magnetic susceptibility. Although the accuracy of our current magnetic separation method is capable of concentrating the substance of interest from a mixture, it is not sufficient to separate the material as a single substance. Further improvements are required to make this equipment practical for industrial and environmental sciences.

Conclusion

The resolution for separating diamagnetic particles was significantly improved by optimizing the performance of the compact magnetic circuit, which was possible by increasing the magnetic force acting on the particle. Specifically, the width of the magnet pole of the circuit was narrowed from 2.0 to 0.8 cm, and the yoke was redesigned in order to increase the magnetic flux density of the experimental area. Accordingly, separation of particles caused by magnetic translation, X_T, was more than doubled compared to the circuit developed in previous studies, and because of the improved resolution, heterogeneous particles that are included in various geological samples are separated using the new apparatus. The techniques developed in the present study serve as a breakthrough in effectively separating regolith-size geological samples with a sufficiently high resolution for practical use. It could also be applied in extracting useful substances as well as in removing harmful ones from industrial wastes.

The program for numerical calculation developed in the present study was effective in confirming the efficiency of a dynamic equation which was introduced to explain the observed results of magnetic translation. The program is effective in improving the accuracy of material identification based on the measured X_T values. It is eligible to design a magnetic circuit with the higher resolution compared to the circuit developed in the present study.

An unidentified particle in mixture could be speedily determined by collating the obtained χ_{DIA} values with a list of published data as described in Table 2 (Uyeda et al. 2019). In contrast to conventional methods such as solution chemical analyses, material identification is performed without sample consumption. Therefore, the device could be developed as an effective pretreatment tool for analyzing various aggregates of heterogeneous particles studied in earth and space science.

Abbreviations

Gra Graphite
Dia Diamond
PP Polypropylene

Acknowledgements

The authors would like to thank Dr. Kohei Fukuda for carefully proofreading the manuscript.

Author contributions

SJ designed and constructed the apparatus, conducted the experiment, prepared all the figures and tables, and wrote 60% of the main text. CU developed the hypotheses of magnetic separation and wrote 20% of the main text. KH contributed to design apparatus and discussion. GT constructed numerical calculation and Figure. KT indicated improved the overall design and structure of the manuscript, and wrote 20% of the main text. All authors discussed the data and reviewed the manuscript.

Funding

Not applicable.

Availability of data and materials

All data generated during this study are available from the corresponding author on reasonable request.

Declarations

Competing interests

The authors declare no competing interests.

Received: 9 November 2023 Accepted: 6 March 2024
Published online: 18 March 2024

References

Anders E. Origin, age, and composition of meteorites. Space Sci Rev. 1964;3:583–714.

Bain GA, Berry JF. Diamagnetic corrections and Pascal's constants. J Chem Educ. 2008;85(4):532.

Gupta R. Diamagnetic susceptibility. In: Landolt-Börnstein new series II, vol. 16. Berlin: Springer. 1983. p. 265-385

Hisayoshi K, Uyeda C, Terada K. Magnetic separation of general solid particles realised by a permanent magnet. Sci Rep. 2016;6(1):38431.

Hitomi M, Yamaguchi W, Hisayoshi K, Uyeda C. Nondestructive method to determine mixing ratio of a binary-mixture particle orientated to investigate material compositions of icy particles in the outer solar system. Planet Space Sci. 2020;183:104580.

Javaux EJ. Challenges in evidencing the earliest traces of life. Nature. 2019;572:451–60.

Jinnouchi S, Hisayoshi K, Uyeda C, Terada K. Magnetization of a diamagnetic particle measured from its parabolic movement caused by field-gradient force in terrestrial gravity. IEEE Trans Magn. 2022;58(2):6000204.

Papike JJ, Simon SB, Laul JC. The lunar regolith: chemistry, mineralogy, and petrology. Rev Geophys. 1982;20(4):761–826.

Pople JA. Molecular-orbital theory of diamagnetism. II. Calculation of Pascal constants for some noncyclic molecules. J Chem Phys. 1962;37(1):60–6.

Uhlen M. Magnetic separation of DNA. Nature. 1989;340(6236):733–4. https://doi.org/10.1038/340733a0.

Uyeda C, Hisayoshi K, Kanou S. Magnetic ejection and oscillation of diamagnetic crystals observed in microgravity. J Phys Soc Jpn. 2010;79(6):064709.

Uyeda C, Hisayoshi K, Terada K. Separation of gold and other rare materials from an ensemble of heterogeneous particles using a NdFeB magnetic circuit. Sci Rep. 2019;9(1):3971.

Watanabe K, Suwa M, Watarai K. New principle of magnetophoretic velocity mass analysis. Anal Sci. 2004;20(11):1483–5.

Yamaguchi C, Hisayoshi K, Hitomi M, Uyeda C, Terada K. Detection of mixing ratio of binary-mixture particles based on a principle of magnetic separation conducted in a microgravity area. AIP Adv. 2020;10(3):035314.

Publisher's Note